Pol. J. Environ. Stud. Vol. 23, No. 2 (2014), 379-384

Original Research

Exploring the Photodegradation of Bisphenol A in a Sunlight/Immobilized N-TiO_2 System

Chao-Yin Kuo*, Ya-Hui Yang

Department of Environmental and Safety Engineering, National Yunlin University of Science and Technology, 123 University Road, Section 3, Douliou, Yunlin 64002, Taiwan

Received: 14 March 2013
Accepted: 19 September 2013

Abstract

Few studies have examined the photodegradation of bisphenol A (BPA) by sunlight/immobilized TiO_2 systems. In this investigation, N-doped TiO_2 (N-TiO_2) was prepared by the calcination of Degussa P25 and urea. The surface characteristics of N-TiO_2 were analyzed by X-ray diffraction, specific surface area analysis, ultraviolent (UV)-vis spectroscopy, Fourier transform infrared spectroscopy (FTIR), scanning electron microscopy (SEM), and X-ray photoelectron spectroscopy (XPS). The photocatalytic activity of the prepared photocatalysts was determined by using them in the photodegradation of BPA under sunlight irradiation. The N-doping of TiO_2 reduced the particle size and band gap of the compound, while increasing the specific surface area and percentage of anatase therein. XPS characterization confirms the substitution of O in the crystal lattice for N species in N-TiO_2, forming O-Ti-N. The BPA degradation rate can be approximated by pseudo-first-order kinetics. At a N/Ti mole ratio of one for N-TiO_2, the rates of BPA photodegradation and mineralization were 0.042 and 0.006 min^{-1}, respectively.

Keywords: photodegradation, bisphenol A, sunlight, TiO_2, N-doping

Introduction

Removal of environmental pollutants by advanced oxidation processes has attracted considerable interest, especially for the TiO_2 system because TiO_2 is nontoxic, has powerful oxidizing activity, and exhibits long-term chemical stability. The effects of TiO_2, TiO_2 loading, ultraviolet (UV) intensity, solution pH, substrate concentration, and the presence of different electron acceptors on UV/TiO_2-related systems has been studied extensively. However, the wide band gap of TiO_2 limits its absorption wavelength to less than 387 nm, capturing only 3-5% of the energy of sunlight and limiting its practical application [1]. Therefore, developing an efficient sunlight-sensitive TiO_2 by narrowing its band gap is an important challenge.

*e-mail: kuocyr@ms35.hinet.net

N-doped TiO_2 (N-TiO_2) [1-5], which extends the spectral response of TiO_2 into the visible-light region, thereby enhancing the photocatalytic activity of TiO_2, has been synthesized in several investigations. Wang and Lim [6], who used visible light to photoexcite N-TiO_2 and Degussa P25 for bisphenol A (BPA) degradation, demonstrated that the removal of BPA after the reaction with N-TiO_2 and Degussa P25 for 2 h were 29% and 5%, respectively. Other than one by Wu et al. [7], no study has examined the photodegradation of BPA using a sunlight/immobilized N-TiO_2 system. Wu et al. [7] immobilized N-TiO_2 in glass balls to form N-TiO_2 glass beads and used them to degrade BPA under irradiation by visible light and sunlight. The ongoing use of BPA in household and commercial products has caused the release of large amounts of BPA into aquatic environments. Owing to its potential disruption of the endocrine function, the presence of BPA in aquatic environments and its poten-

tial adverse effects on ecological and public health have attracted much attention. Accordingly, BPA was utilized herein as the parent compound to evaluate the photocatalytic activity of immobilized N-TiO_2 under irradiation by sunlight. The objectives of this study are to:

(i) characterize prepared TiO_2 and N-TiO_2 particles
(ii) compare the photocatalytic activity of TiO_2 and N-TiO_2 in BPA degradation under irradiation by sunlight
(iii) determine the effects of the amount of N-doping
(iv) to assess the repeatability of the use of the immobilized N-TiO_2 system for BPA degradation.

Materials and Methods

Materials

Commercial Degussa P25 powder was used as obtained. The N source was urea (Merck). The modulator used in the formation of immobilized photocatalysts was SiO_2 (PPG Industries). The parent compound, BPA, was obtained from Sigma-Aldrich. The pH of the solution was adjusted using HNO_3 and NaOH. All chemicals were analytical reagent grade and used as received.

Experimental Methods

In preparing N-TiO_2, 100 g Degussa P25 was ground with urea (3.79, 18.95, and 37.9 g) and mixed with deionized water. To the mixture was added 1% (wt.) SiO_2; the mixture was then thoroughly mixed, and then shaped under pressure to form N-TiO_2 balls. The N-TiO_2 balls were first dehydrated at 105ºC and finally calcined at 450ºC for 8 h. The N/Ti mole ratios were 0.1, 0.5, and 1.0 and the corresponding prepared immobilized N-TiO_2 was denoted as 0.1 NTS, 0.5 NTS, and 1.0 NTS, respectively. Using the same procedures as above, but without adding urea, Degussa P25, denoted as T herein, was used as a standard material to compare its photocatalytic activity with that of the prepared N-TiO_2 for BPA photodegradation.

The crystalline structure of the prepared photocatalysts was analyzed by X-ray diffraction (XRD) (Rigaku TTRAX-III, Japan). The accelerating voltage and applied current were 40 kV and 30 mA, respectively. The XRD patterns were recorded with 2θ values in the range of 20-80º. The specific surface area of samples was determined using nitrogen as the adsorbate at 77 K in a static volumetric apparatus (Micromeritics ASAP 2020, USA). UV-vis spectroscopy (Jasco V-670, Japan) was utilized to obtain the absorbance spectra of the photocatalysts at wavelengths of 200-800 nm. The UV-vis diffuse reflectance spectra were used to calculate the band gap energy of the photocatalysts. The morphology of the prepared photocatalysts was elucidated by scanning electron microscopy (SEM) (JEOL 6330 TF, Japan). The functional groups of photocatalysts were identified by Fourier transform infrared spectroscopy (FTIR) using a Spectrum One and Autoimagic system (Perkin Elmer) via the KBr pressed-disc method. The X-ray photoelectron spectroscopic (XPS) measurements were made using a Vacuum Generator ECSALAB photoelectron spectrometer (East Grinsted) with a monochromatic Al Kα (1486.6 eV) X-ray source. The carbon 1s peak at 284.5 eV was used to calibrate the spectra. The BPA concentration was measured using a high-performance liquid chromatograph (HPLC) with a UV detector (Agilent Technologies 1200 Series, USA). The UV detector was set to detect the wavelength 197 nm. Separations were performed in a Supelcosil C18 column (Supelco). The mobile phase was Milli-Q water that was combined with CH_3CN (40:60 v/v) at a flow rate of 0.5 mL/min. Injection volume was 20 μL. The decrease in total organic carbon (TOC), measured using a TOC analyzer (O.I. 1010; USA), revealed BPA mineralization.

The photocatalytic reactor comprised four 30 cm-long quartz tubes. Each tube had an external diameter of 1.2 cm and an internal diameter of 1 cm. The column photo-reactor was used as in Wu et al. [7]. Each quartz tube was filled with 8.1-9.3 g N-TiO_2 balls before 10 mg/L BPA solution was added to the system using a peristaltic pump (SJ-1211H, Bioinstrument ATTA). A total of 26.4-30.9 g TiO_2 (excluding SiO_2 and urea) was present in the photocatalytic reactor. The optimal experimental pH for BPA degradation in the sunlight/TiO_2 system was 6 [8]; therefore, the initial solution pH was set to 6. The flow rate of the BPA solution was maintained at 1.5 mL/min. The residence time of the BPA solution in the reactor was 61 min. The column photo-reactor was irradiated with sunlight (am 11:30-pm 12:31) at room temperature. The intensity of the sunlight was 67.8-70.7 mW/cm^2. The photocatalytic efficiency of BPA was evaluated in cyclic tests (run 1 to run 5) using 1.0 NTS under the same conditions. Some experiments were conducted in triplicate and average values are reported.

Results and Discussion

Surface Characteristics of Photocatalysts

Fig. 1 shows the XRD patterns of the prepared photocatalysts. The anatase content was determined from the

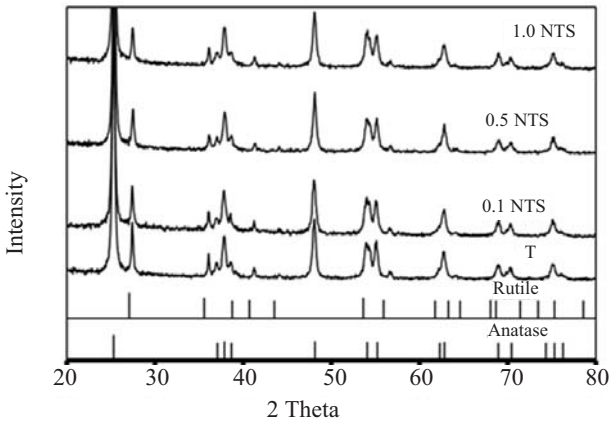

Fig. 1. XRD pattern of prepared photocatalysts.

Table 1. Characteristics of prepared photocatalysts.

Photocatalysts	T	0.1 NTS	0.5 NTS	1.0 NTS
Anatase (%)	75.5	76.6	77.1	78.8
Rutile (%)	24.5	23.4	22.9	21.2
Particle size (nm)	37	33	31	31
BET (m^2/g)	45.6	47.8	45.7	49.4
Band gap (eV)	3.1	3.0	3.0	3.0
k (min^{-1})	0.018	0.019	0.031	0.042
R^2	0.989	0.987	0.988	0.965

intensity of (1 0 1) anatase diffraction, IA, and that of (1 1 0) rutile diffraction, IR, using Eq. (1) [9]. From the XRD patterns, the crystalline size of the prepared powders was calculated using the Scherrer formula, Eq. (2):

$$\text{Anatase (\%)} = \frac{1}{1+12.6\frac{I_A}{I_R}} \times 100 \quad (1)$$

$$D = \frac{0.9\lambda}{\beta \cos\theta} \quad (2)$$

...where D is crystalline size in nm; λ denotes the wavelength of the X-rays (0.15418 nm); β is the line width of the anatase (1 0 1) and rutile (1 1 0) peaks at the half maxima, and θ is the diffraction angle [10]. The diffraction peaks of various crystal planes of anatase, were 25.4º (1 0 1), 37.9º (0 0 4), 48.1º (2 0 0), 55º (2 1 1), and 62.5º (2 0 4) (JCPDS No. 21-1272). Other diffraction peaks at 27.4º, 36.1°, 41.2°, and 54.3° corresponded to the (1 1 0), (1 0 1), (1 1 1), and (2 1 1) planes of the crystalline phase of rutile, respectively (JCPDS No. 21-1276). Table 1 lists the surface characteristics of the prepared photocatalysts. The anatase percentage increased from 76% to 79% as the N-doping amount increased. The XRD diagrams reveal that N-doping retards transformation of the TiO_2 phase from anatase to rutile. This retardation may be caused by stabilization of the anatase phase by surrounding N ions. The TiO_2 with the anatase crystalline structure exhibited a higher photocatalytic activity than TiO_2 with another crystalline structure, such as rutile or brookite. 1.0 NTS may have the highest photocatalytic activity.

The particle size of T was greater than that of N-TiO_2; conversely, the surface area of T was smaller than that of N-TiO_2 (Table 1). The band gaps of T and 1.0 NTS were 3.1 and 3.0 eV, respectively, as determined from UV-vis measurements. Xiang et al. [4] indicated that N-doping induced a red-shift of the absorption edge from 0.08 to approximately 0.8 eV. This study found similar experimental results. The red shift means that the N-TiO_2 could be excited to generate additional hole-electron pairs under irradiation by visible light, increasing its photocatalytic activity. Silveyra et al. [3] found that N-doping reduced the band gap energy of TiO_2 from 3.01 to 2.88 eV. Rengifo-Herrera et al. [11] found that the band gap energies of Degussa P25 and the Degussa P25/urea composite were 3.10 and 2.73 eV, respectively. Asahi et al. [2] and Xing et al. [1] showed that N-doping effectively reduced the band gap of TiO_2 by generating an isolated N 2p narrow band above the O 2p valence, which was formed by the incorporation of N atoms into the TiO_2 lattice.

Fig. 2 displays SEM micrographs of the prepared N-TiO_2. The prepared N-TiO_2 mostly consisted of spherical nanoparticles with a high tendency to agglomerate and form a porous structure. The aggregates in N-TiO_2 were 30-33 nm (Fig. 2). Fig. 3 presents the FTIR spectra of photocatalysts that were obtained with different urea concentrations. Three major absorbance peaks were observed at 1,108, 1,639, and 3,392 cm^{-1}. The absorption peak at 1,630 cm^{-1} corresponded to the Ti-O structure, and the absorption peak at 3,400 cm^{-1} was assigned to the OH species [12]. The FTIR spectra of the N-doped TiO_2 included a hyponitrite peak at 1,104 cm^{-1} [13]. Peng et al. [14] showed that a new peak, around 1,110 cm^{-1}, that appeared in N-doped TiO_2 was attributable to the formation of hyponitrite. However, the FTIR analysis in both this study and that of Wu et al. did not identify the N atoms that were incorporated into the TiO_2 crystal lattice [7].

Figs. 4(a-c) display the XPS spectra of N 1s, Ti 2p, and O 1s for the prepared photocatalysts, respectively. The peak at 399 eV was attributed to anionic N in O-Ti-N linkages by Asahi et al. [2]. Another peak at a higher binding energy of 401 eV for the N 1s region of N-TiO_2 was attributed to oxidized N in Ti-O-N. Xing et al. [1] characterized oxidized N in Ti-O-N as chemically adsorbed onto the catalyst surface and appeared at the high binding energy of 401 eV in N 1s XPS spectra. Xiang et al. [4] suggested that the N 1s peak

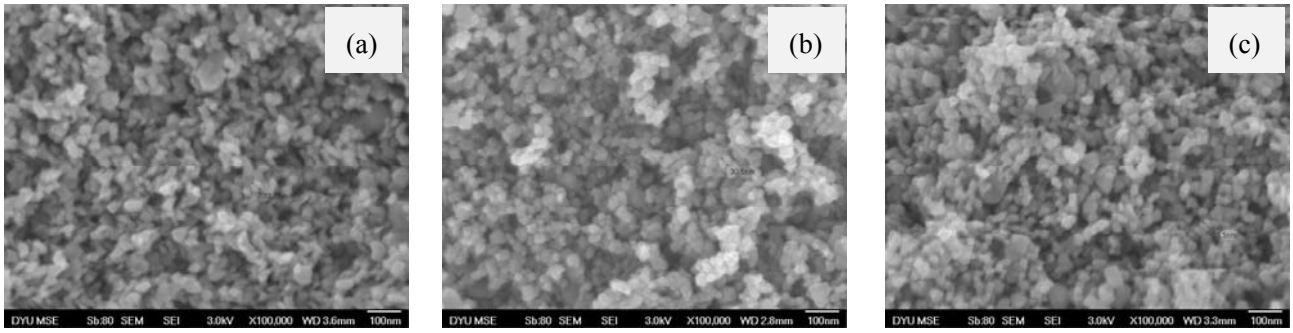

Fig. 2. SEM micrographs of prepared N-TiO_2 (a) 0.1 NT, (b) 0.5 NT, (c) 1 NT.

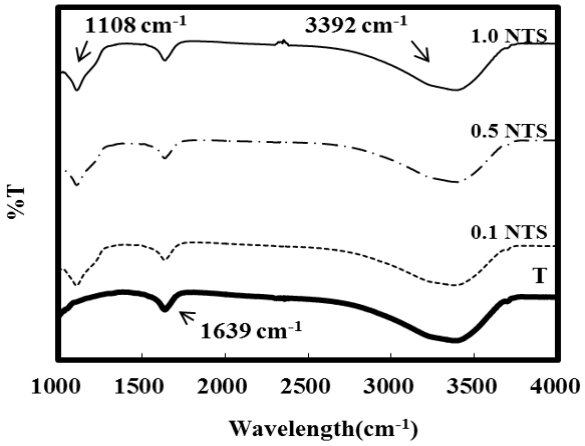

Fig. 3. FRIR spectra of prepared photocatalysts.

at 400 eV is likely the N- anion incorporated into the TiO_2 lattice, as O-Ti-N, Ti-O-N and/or Ti-N-O structural features. The Ti 2p3/2 and Ti 2p1/2 spin-orbital splitting photoelectrons were located at binding energies of 458.6 and 464.4 eV, respectively, and were attributed to Ti^{4+} (TiO_2) [15]. Peaks at 529.4 and 530.3 eV were assigned to O 1s; the former can be attributed to TiO_2 and the latter to absorbed hydroxyl groups [15]. The peak at 531.4 eV was attributed to the presence of Ti-O-N bonds. Based on these observations (Fig. 4), N doping in TiO_2 may be present in O-Ti-N.

Photodegradation of BPA

Figs. 5(a) and (b) display BPA removal in background and photocatalytic experiments, respectively. The percentages of BPA removed by adsorption using T, 0.1 NTS, 0.5 NTS, and 1.0 NTS after 61 min were 17%, 45%, 28%, and 19%, respectively (Fig. 5a). Those removed by photodegradation for the same period were 81%, 82%, 88%, and 95%, respectively (Fig. 5b). The BPA photodegradation rate satisfies pseudo-first-order kinetics, and various studies have demonstrated that photodegradation rates for BPA can be approximated using pseudo-first-order kinetics [5, 16]. The BPA photodegradation rate constants for T, 0.1 NTS, 0.5 NTS, and 1.0 NTS was 0.018, 0.019, 0.031, and 0.042 min^{-1}, respectively. Photocatalytic activity was significantly improved by N-doping. Yang et al. [5] demonstrated that the percentages of BPA removed by P25 and N-TiO_2 under irradiation by visible light in a suspended system were 15% and 30%, respectively; these BPA removal percentages are similar to those obtained herein. The amounts of BPA removed by adsorption followed the order 0.1 NTS > 0.5

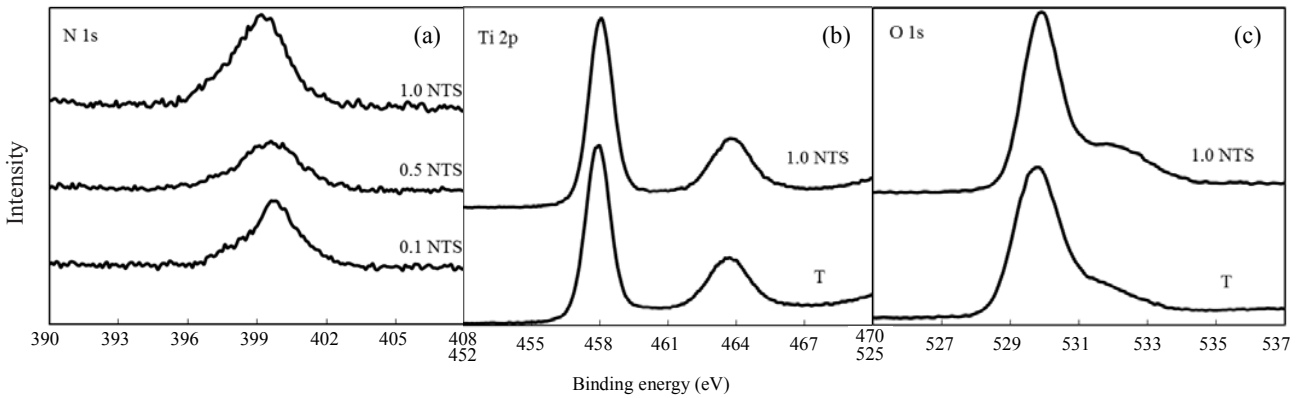

Fig. 4. XPS spectra of prepared photocatalysts (a) N 1s, (b) Ti 2p, (c) O 1s.

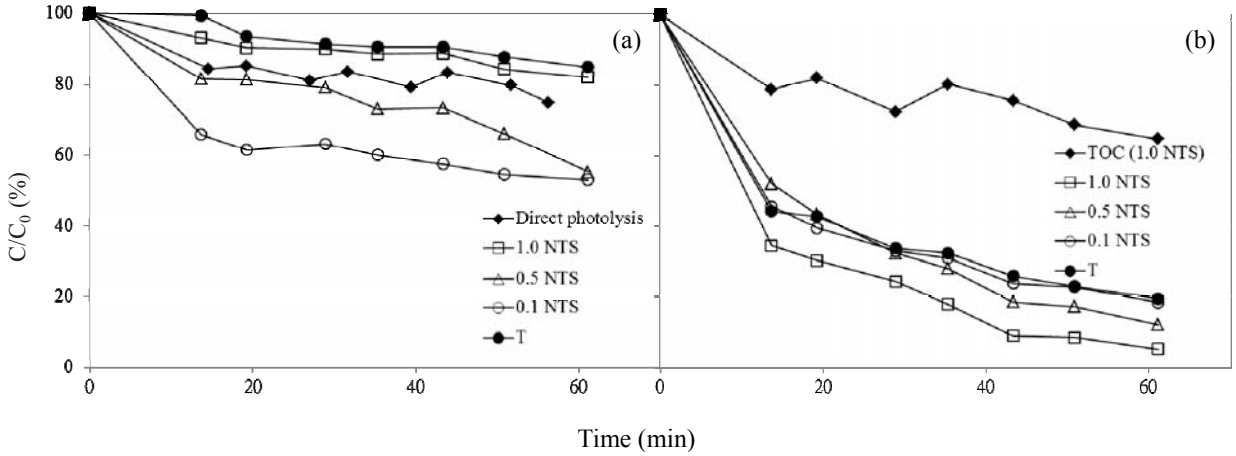

Fig. 5. Removal of BPA (a) background experiments, (b) photocatalytic experiments.

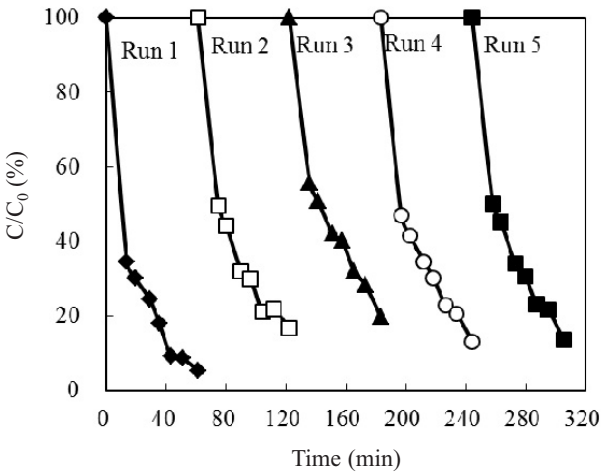

Fig. 6. Photocatalytic efficiency of cyclic tests for 1.0 NTS.

NTS > 1.0 NTS > T; those by photodegradation followed the order 1.0 NTS > 0.5 NTS > 0.1 NTS > T. Wu et al. [7] obtained adsorption and photodegradation percentages of BPA by reaction with 0.1 NTS for 61 min of 12% and 91%, respectively, and corresponding values for reaction with 0.5 NTS of 11% and 88%, respectively. The BPA adsorption percentage herein exceeded that obtained by Wu et al. [7]; however, Wu et al. [7] obtained a higher BPA photodegradation percentage and rate than were obtained in this study. Despite the importance of adsorption as a mechanism for BPA removal, adsorption is not the main mechanism thereof. We suggest that the bonding between N and TiO_2 particles in photodegradation may play a key role in BPA removal. Asahi et al. [2] suggested that N dopants can synergistically function as electron traps that inhibit the recombination of photogenerated electron-hole pairs in the N-TiO_2 system, enhancing the photodegradation efficiency of N-TiO_2.

Wu et al. [7] employed ethyl titanate and urea to generate N-TiO_2. The etched glass balls were immersed in a 5% (w/v) N-TiO_2 solution and conditioned at 120ºC for 12 h to form immobilized N-TiO_2/glass beads. The immobilized N-TiO_2/glass beads thus formed were applied to degrade BPA under irradiation by sunlight. For 0.1 NT and 0.5 NT, the anatase phase and band gap of N-TiO_2 herein were higher than those obtained by Wu et al. [7]. However, the BPA removal rate that was obtained by Wu et al. [7] exceeded that in this study. Wu et al. [7] used sol-gel/microwave and calcination methods to generate immobilized N-TiO_2, and these procedures of preparation were more complex than those used in this work. This study developed a simple method to produce immobilized N-TiO_2, which exhibited acceptable efficiency in removing BPA.

The TOC and BPA removal rate of 1.0 NTS was 0.006 and 0.042 min^{-1}, respectively (Fig. 5b). Several studies of BPA photodegradation by TiO_2 have suggested that the roles of hydroxyl radicals and BPA degradation are mainly through demethylation and hydroxylation due to the generation of hydroxyl radicals [8, 17]. Phenol, p-hydroquinone, p-isopropenylphenol, p-hydroxybenzaldehyde, and 4-hydroxyphenyl-2-propanol are intermediate products of the photodegradation of BPA in the UV/TiO_2 system [17, 18]. Analyses of microtox toxicity by Chiang et al. [19] revealed that the intermediates that are formed by BPA photodegradation in UV/TiO_2 and UV/Pt-TiO_2 systems were less toxic than BPA. Wang and Lim [20], who used visible-light irradiation to photoactivate C-N-codoped TiO_2 for BPA photodegradation, found that the BPA solution was nearly non-toxic after four hours of irradiation. Kaneco et al. [8] identified the final degradation product in the sunlight/TiO_2 system as carbon dioxide. As the formation of intermediates from the photocatalytic degradation of BPA is independent of the form of TiO_2 used [19], the photodegradation pathways and byproducts of BPA in this study are similar to those identified by Watanabe et al. [17] and Horikoshi et al. [18].

Fig. 6 plots the photocatalytic efficiency of 1.0 NTS in cyclical tests. The extent of BPA removal in runs 1, 2, 3, 4, and 5 were 95%, 83%, 80%, 87%, and 87%, respectively. Photocatalytic efficiency declined slightly as the number of repeats increased, suggesting that the immobilized N-TiO_2 system was stable during photocatalytic degradation under irradiation by sunlight.

Conclusions

In this study, N-TiO_2 was utilized to photodegrade BPA under irradiation by sunlight in an immobilized system. The effects of the N/Ti ratio in N-TiO_2 on BPA photodegradation were evaluated. Doping TiO_2 with N increased the specific surface area and percentage of anatase and reduced the particle size and band gap. Experimental results reveal that the chemical states of N-doped TiO_2 were those of O-Ti-N. Experimental results also indicate that the adsorption effect is not the main influence in BPA removal, and that the connection between N and TiO_2 particles for photodegradation may play a key role in BPA removal. The rate of BPA removal increased with the amount of N doping.

Acknowledgements

The authors would like to thank the National Science Council of the Republic of China, Taiwan, for financially supporting this research under Contract No. NSC 101-2221-E-151-038-MY3.

References

1. XING M., ZHANG J., CHEN F. New approaches to prepare nitrogen-doped TiO_2 photocatalysts and study on their photocatalytic activities in visible light. Appl. Catal. B-Environ. **89**, 563, **2009**.
2. ASAHI R., MORIKAWA T., OHWAKI T., AOKI K., TAGA Y. Visible-light photocatalysis in nitrogen-doped titanium oxides. Science **293**, 269, **2001**.

3. SILVEYRA R., SAENZ L.T., FLORES W.A., MARTINEZ V.C., ELGUEZABAL A.A. Doping of TiO_2 with nitrogen to modify the interval of photocatalytic activation towards visible radiation. Catal. Today **107-108**, 602, **2005**.
4. XIANG X., CHEN M., JU Y.F., ZU X T., WANG L.M., ZHANG Y. N-TiO_2 nanoparticles embedded in silica prepared by Ti ion implantation and annealing in nitrogen. Nucl. Instrum. Meth. B. **268**, 1440, **2010**.
5. YANG J., DAI J., LI J. Synthesis, characterization and degradation of bisphenol A using Pr, N co-doped TiO_2 with highly visible light activity. Appl. Surf. Sci. **257**, 8965, **2011**.
6. WANG X., LIM T.T. Solvothermal synthesis of C-N codoped TiO_2 and photocatalytic evaluation for bisphenol A degradation using a visible-light irradiated LED photoreactor. Appl. Catal. B-Environ. **100**, 355, **2010**.
7. WU C.H., KUO C.Y., LIN C.J., CHIOU P.K. Preparation of N-TiO_2 using a microwave/sol-gel method and its photocatalytic activity for bisphenol A under visible-light and sunlight irradiation. Int. J. Photoenergy **2013**, 1, **2013**.
8. KANECO S., RAHMAN M.A., SUZUKI T., KATSUMATA H., OHTA K. Optimization of solar photocatalytic degradation conditions of bisphenol A in water using titanium dioxide. J. Photoch. Photobio. A. **163**, 419, **2004**.
9. SPURR R.A., MYERS H. Quantitative analysis of anatase-rutile mixtures with an X-ray diffractometer. Anal. Chem. **29**, 760, **1957**.
10. KANG I.C., ZHANG Q., YIN S., SATO T., SAITO F. Preparation of a visible sensitive carbon doped TiO_2 photocatalyst by grinding TiO_2 with ethanol and heating treatment. Appl. Catal. B-Environ. **80**, 81, **2008**.
11. RENGIFO-HERRERA J.A., KIWI J., PULGARIN C. N, S co-doped and N-doped Degussa P-25 powders with visible light response prepared by mechanical mixing of thiourea and urea. Reactivity towards E. coli inactivation and phenol oxidation. J. Photoch. Photobio. A. **205**, 109, **2009**.
12. LI H., LI J., HUO Y. Highly active TiO_2N photocatalysts prepared by treating TiO_2 precursors in NH_3/ethanol fluid under supercritical conditions. J. Phys. Chem. B. **110**, 1559, **2006**.
13. SAKTHIVEL S., JANCZAREK M., KISCH H. Visible light activity and photoelectrochemical properties of nitrogen-doped TiO_2. J. Phys. Chem. B. **108**, 19384, **2004**.
14. PENG F., CAI L., YU H., WANG H., YANG J. Synthesis and characterization of substitutional and interstitial nitrogen-doped titanium dioxides with visible light photocatalytic activity. J. Solid State Chem. **181**, 130, **2008**.
15. ZHANG X., ZHOU M., LEI L. Preparation of an Ag-TiO_2 photocatalyst coated on activated carbon by MOCVD. Mater. Chem. Phys. **91**, 73, **2005**.
16. KUO C.Y., WU C.H., LIN H.Y. Photocatalytic degradation of bisphenol A in a visible light/TiO_2 system. Desalination **256**, 37, **2010**.
17. WATANABE N., HORIKOSHI S., KAWABE H., SUGIE Y., ZHAO J., HIDAKA H. Photodegradation mechanism for bisphenol A at the TiO_2/H_2O interfaces. Chemosphere **52**, 851, **2003**.
18. HORIKOSHI S., TOKUNAGA A., HIDAKA H., SERPONE N. Environmental remediation by an integrated microwave/UV illumination method: VII. Thermal/non-thermal effects in the microwave-assisted photocatalyzed mineralization of bisphenol-A. J. Photoch. Photobio. A. **162**, 33, **2004**.
19. CHIANG K., LIM T.M., TSEN L., LEE C.C. Photocatalytic degradation and mineralization of bisphenol A by TiO_2 and platinized TiO_2. Appl. Catal. A-Gen. **261**, 225, **2004**.
20. WANG X., LIM T.T. Effect of hexamethylenetetramine on the visible-light photocatalytic activity of C-N codoped TiO_2 for bisphenol A degradation: evaluation of photocatalytic mechanism and solution toxicity. Appl. Catal. A-Gen. **399**, 233, **2011**.